Excitation of Ar lines in the cathode region of a dc discharge

K. Rózsa* and A. Gallagher
Joint Institute for Laboratory Astrophysics, University of Colorado and National Institute of Standards and Technology, Boulder, Colorado 80309-0440

Z. Donkó
Research Institute for Solid State Physics, P.O. Box 49, H-1525 Budapest, Hungary
(Received 24 February 1995)

Measurements of the spatial distribution of different Ar lines are reported for a flat cold cathode discharge in the j/P^2 range of 10^{-4} to 10^{-2} A cm^{-2} mbar^{-2}, where j is the current density and P is the pressure. In this range, excitation by heavy particles and by electrons can be studied since they produce a cathode glow and a negative glow that are well separated. With increasing j/P^2 the heavy-particle excitation and the cathode glow increase, while the negative glow extends to a larger distance. The voltage, the pressure (P) times the lengths of the cathode glow and the cathode sheath, and the fraction of the input energy that goes into the negative glow and the cathode glow have a dependence on j/P^2 that is independent of pressure. We also report data on the decay of the negative glow beyond its peak, but this decay length times pressure has a dependence on j/P^2 that changes with pressure. The measured voltage and lengths are compared to previous data and to a recent calculation.

PACS number(s): 52.20.Fs, 52.20.Hv, 52.25.Rv

I. INTRODUCTION

There has been a continuous interest in the cathode region of glow discharges over the last 70 years. More recently, this part of the discharge has been extensively used for applications like cathode sputtering, plasma deposition, analytical chemistry, hollow cathode lamps, and lasers [1–7]. For a better understanding of cathode region phenomena a number of experiments and modeling studies have been performed [8–10].

In the present work we investigated a low-pressure, $P=0.13$–0.67 mbar (0.99 bar$=10^5$ Pa), Ar discharge near a cold cathode surface. We performed spatial scans of several spectral lines from the cathode surface through the negative glow. These intensity distributions contain a "cathode glow" component, attributed to heavy-particle collisions, that peaks at the cathode, and a "negative glow" component, attributed to electron-atom collisions, that peaks ~ 1 cm from the cathode. In the j/P^2 range we have investigated (5×10^{-5}–10^{-2} A cm^{-2} mbar^{-2}) the cathode glow and the negative glow are well separated from each other. We present measurements on the peak and total intensities in these two parts of the discharge, as well as the behavior of the distance to the negative glow peak and the decay of the negative glow beyond this peak.

II. EXPERIMENTAL ARRANGEMENT

The experimental arrangement can be seen in Fig. 1. A flat, air-cooled 43 mm diameter Cu cathode was placed into a $4\frac{1}{2}$ in. flange, six-way metal cross that was evacuated through a butterfly valve by a turbomolecular pump. Argon flowed continuously during the measurements to maintain cleanliness. Except for the front surface, all parts of the cathode were protected either by Teflon insulators or by a floating metal shield near the cathode surface (Teflon was shielded from direct discharge radiation). The image of the discharge was projected onto the 0.1 mm wide, 1.5 mm high entrance slit of a monochromator with 0.22 magnification. With a 4 cm aperture the lens collected 0.06 radian of light from the discharge. The combination of the angular divergence and slit magnification gave a spatial resolution at the discharge of about 1 mm perpendicular and 7 mm parallel to the cathode surface. The lens was translated by a stepping motor, thus translating the discharge image on the plane of the entrance slit. The vacuum window allowed us to study about 50 mm of discharge length, which was scanned in 400 steps. The stepping motor was driven by a personal computer which also recorded the optical signal from the photomultiplier.

Scanning the lens introduces a sensitivity variation with position. Projecting a small part of the discharge onto an optical fiber which can be translated together with the lens would be free of this, but it provides much less light into the monochromator. The present method allowed scans in a few minutes with reasonable signal to noise, even at low current densities.

The linearity of the spatial scan was checked with a row of 1 mm holes in the front of the discharge, and found satisfactory. We measured the sensitivity of the system, versus position along the scan, by measuring the light from a positive column lamp in the place of the discharge. This has a constant intensity along its length, whereas we measured a slow decrease of 25% from the

*Permanent address: Research Institute for Solid State Physics, P.O. Box 49, H-1525 Budapest, Hungary.

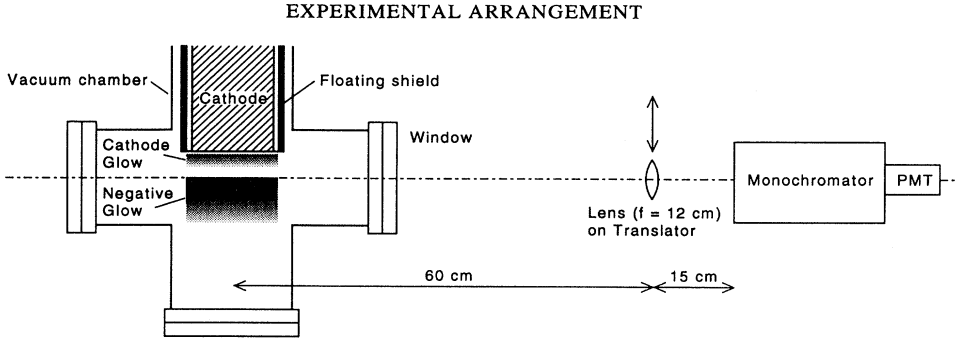

FIG. 1. Experimental arrangement for measuring spatial intensity distribution of different spectral lines. The cross section of the discharge region is drawn approximately to scale, but the optics are diagrammatic.

cathode to the other end of our measurement (the end of the window). We have corrected our measurements for this, as well as the varying spectral sensitivity of the monochromator and the photomultiplier tube detector, obtained by scanning a standard tungsten-iodide lamp spectrum.

III. RESULTS

The spectrum of the negative glow and the cathode glow were recorded for 0.27 mbar pressure and 8 mA current. Intensities of lines in the blue and the infrared part of the spectrum $x=2$ cm from the cathode in the negative glow (NG), and at the cathode glow peak (KG), recorded through a logarithmic amplifier, are shown in Fig. 2. Variations of line intensities for these two parts of the spectra, due to the different dominant excitation processes, are clearly noticeable. For example, in the cathode glow the 8115 line is about a factor of 3 stronger than the 7503 line, while in the negative glow the ratio is reversed.

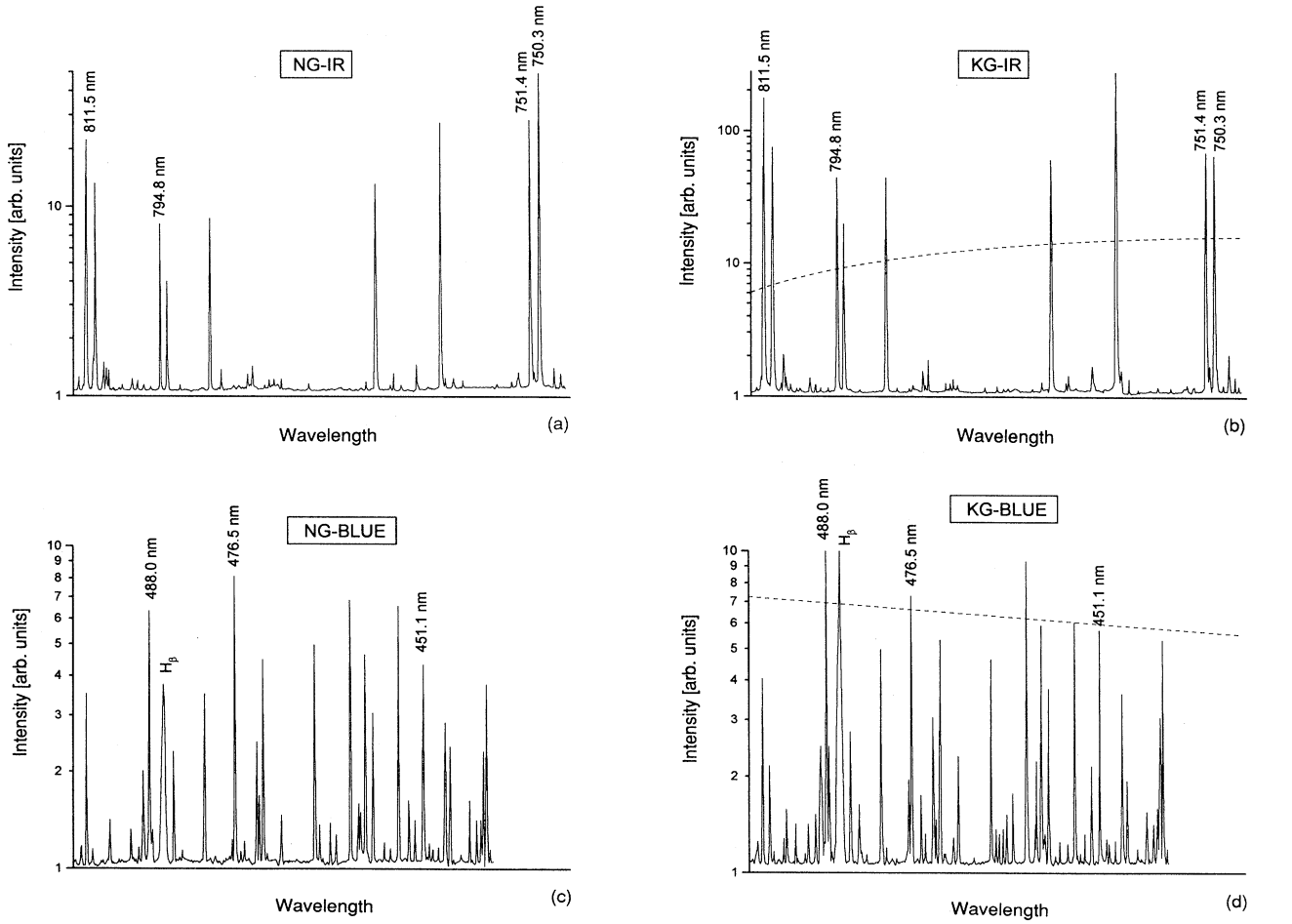

FIG. 2. The blue-green and the infrared part of the spectrum from the negative glow (NG) and the cathode glow (KG), for 8 mA current and 0.27 mbar pressure. The relative spectral sensitivity is shown as a dashed line, but the IR sensitivity has been multiplied by 10 to fit on the graph.

The identified lines are used later in this paper. The same intensity units are used for all of the data of Fig. 2, but these spectra have not been corrected for the spectral sensitivity of the monochromator and photomultiplier. This relative sensitivity is shown in Fig. 2, and the corrected intensity ratios for the different spectral lines can be seen in Fig. 3.

The full spatial dependence of six Ar lines 811.5, 794.8, 751.4, 750.3, 696.5, and 451.1 nm from $4P_9$, $4P_4$, $4P_5$ $4P_1$, $4P_2$, and $5P_5$ states, and two Ar^+ lines, 488.0 and 476.5 nm from $4p(^2D^o)$ and $4p\ ^2P$ states were then measured versus x, the distance from the cathode, for a range of pressures and currents. The spatial dependences of four of these lines are shown in Fig. 3. These are representative of all eight lines, so only four are reported here. Two of these lines (811.5 and 750.3 nm) were chosen to connect with the data of Scott and Phelps, who have shown that these have very different heavy-particle excitation rates [11]. The other two (451.1 and 476.5 nm) represent a higher level of Ar and ~20 eV excited Ar^+. The negative glow was present in all eight lines, as was the cathode glow at high j/P^2 values. The cathode glow/negative glow intensity ratio is the largest for the 811.5 nm line, and then decreases in the following order: 794.8, 696.5, 751.4, 750.4, 451.1, 488.0, and 476.5 nm.

The cathode glow peaks at the cathode surface ($x=0.8$ mm in Fig. 3), but due to the spatial resolution in this data the recorded peak occurs at $x=1.5$ mm. (A measurement of the entire spectrum, taken with a video camera with ~0.1 mm spatial resolution, showed a nearly linear intensity increase to the cathode surface.) For all lines the cathode glow peak (at $x=1.5$ mm) increases more rapidly than the negative glow peak (at $x=8-20$ mm) with increasing current. For all of the lines, it can clearly be seen that with increasing current density, the gap between the negative and cathode glow (i.e., the cathode dark space) shrinks while the negative glow intensity falls more gradually beyond the peak.

Figure 4 shows the intensity distribution of the 750.3 mm line for 4 mA at two different pressures. It is a general behavior that with decreasing pressure the cathode and negative glow decay lengths increase and the intensity of the cathode glow increases relative to the negative glow. Figure 5 shows the Pd value (P is the gas pressure and d is the distance to the negative glow peak), the voltage and E_0/N (N is the gas density and E_0 is the electric field at the cathode surface) as a function of j/P^2. Data at three pressures are included here, and this agreement indicates j/P^2 scaling. We obtained E_0/N by assuming linear decay of the electric field from the cathode to the

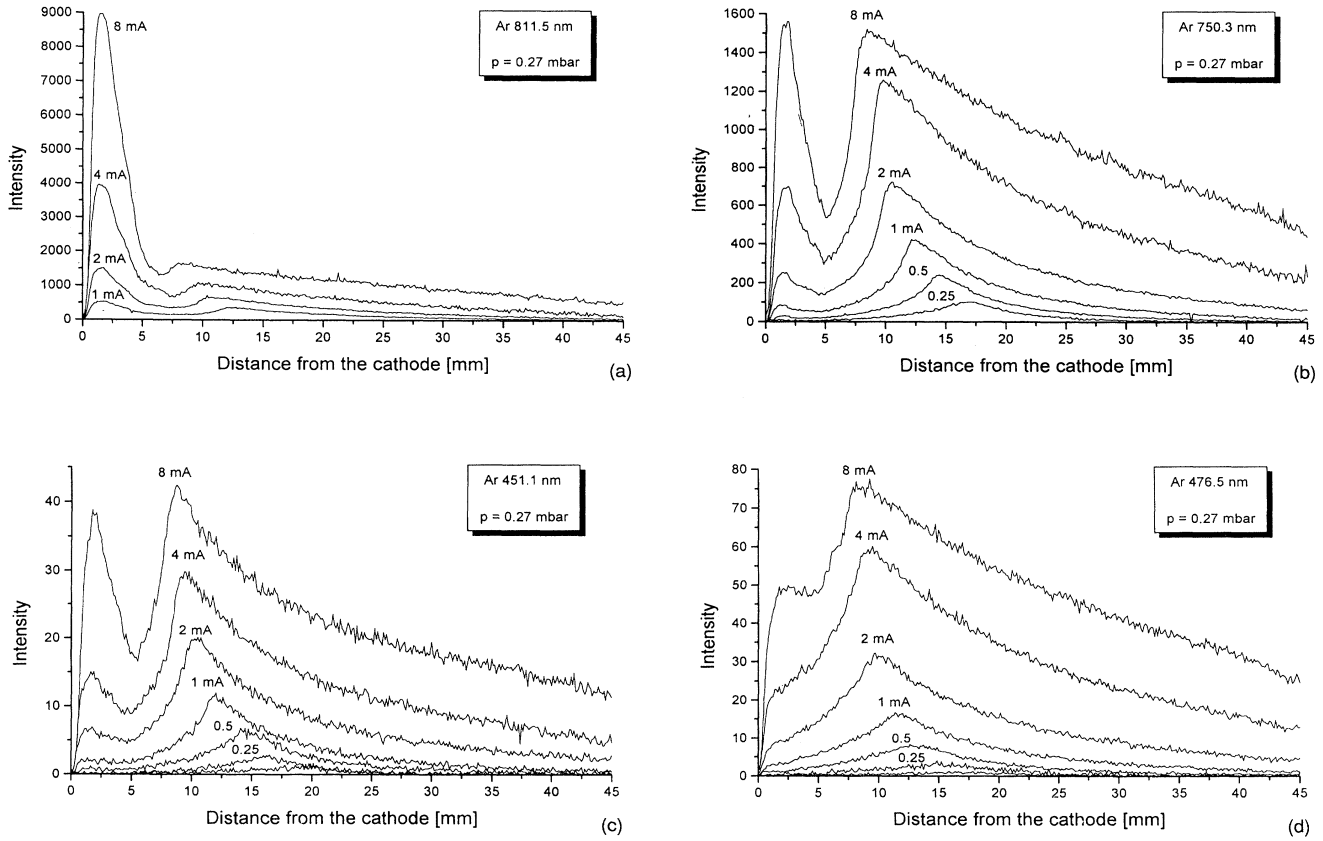

FIG. 3. Spatial dependence of the intensity for different spectral lines vs distance from the cathode at 0.27 mbar: (a) 811.5 nm, (b) 750.3 nm, (c) 451.1 nm (atomic transitions), (d) 476.5 nm (ionic line). The spatial resolution is ~1 mm and the cathode edge is at +0.7 mm.

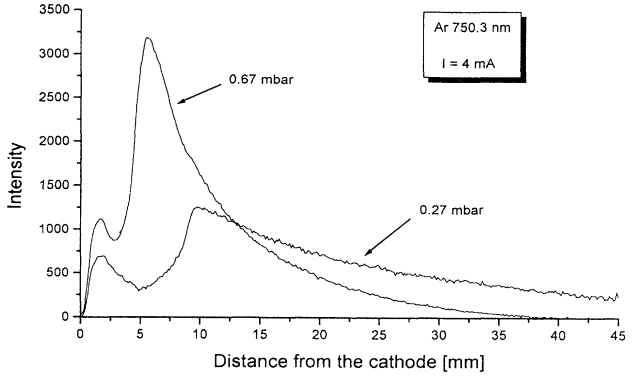

FIG. 4. Spatial intensity dependence of the 750.3 nm line for two different (0.27 and 0.67 mbar) pressures. $I=4$ mA.

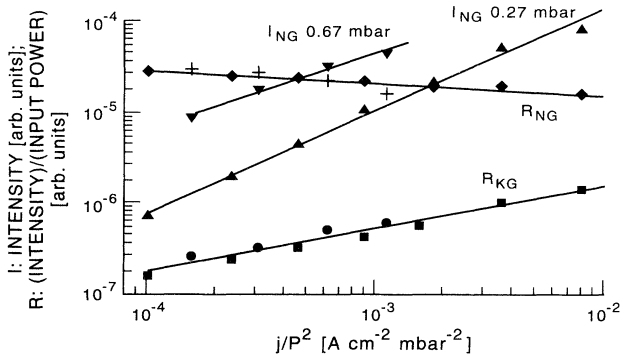

FIG. 6. The total (spatially integrated) negative glow intensity I_{NG} of the 750.3 nm line vs j/P^2, at 0.67 and 0.27 mbar, respectively. The same data are plotted as $R_{NG}=I_{NG}/W$ where W is the input electrical power (+ and ◆). Similarly, $R_{KG}=I_{KG}/W$ for the same two pressures.

negative glow peak [12,13] and negligible voltage drop from there to the anode. The voltage varies approximately as $(j/P^2)^{0.25}$, E_0/N as $(jP^2)^{0.45}$, and Pd as $(j/P^2)^{-0.2}$. For comparison, the average voltages measured by Druyvesteyn with a graphite cathode [12] and Klyarfeld, Guseva, and Porkrovskaya-Sobleva with a Cu cathode [13] are also shown by the dashed curves. This is a selection from many values in the literature; most indicate higher voltages than in these two references. The voltage is very sensitive to the secondary electron emission coefficient, hence to the condition and cleanliness of the cathode surface, as well as to gas impurities that can be Penning ionized by argon metastables.

Note in Fig. 3 that the peak intensity of the negative glow tends to saturate with increasing current, but the negative glow decays more slowly beyond the peak as the current increases. As a result, the spatially integrated ("total") negative glow intensity, which we label I_{NG} does not saturate. This behavior is seen for all lines investigated, and is shown in Fig. 6 for the 750.3 nm line at two pressures. Here I_{NG} includes an exponentially decaying extrapolation beyond the end of the observed region, with decay length L ($I_{NG} \propto e^{-x/L}$). These two sets of I_{NG} data grow approximately linearly with j/P^2, but they yield different curves at different pressures. However, the ratio $R_{NG}=I_{NG}/W$ where W is the discharge power has a dependence on j/P^2 that is independent of pressure, as seen in Fig. 6. The gradual decrease of R_{NG} with increasing j/P^2, roughly proportional to $(j/P^2)^{-0.1}$ in Fig. 6, is also seen for three other lines in Fig. 7.

The cathode glow always appears peaked at the cathode surface, within our spatial resolution, and the intensity falls approximately linearly with distance from the cathode [see Fig. 3(a)]. Defining L_K as the position where a linear extrapolation reaches zero, we find that L_K is nearly independent of current (Fig. 3) and $PL_K \cong 0.10$ mbar cm is essentially independent of pressure. Defining I_{KG} as the spatially integrated intensity of the cathode glow and $R_{KG}=I_{KG}/W$, we find that I_{KG} as a function of j/P^2 is pressure dependent, whereas R_{KG} is not. R_{KG} for the 750.3 nm line is shown in Fig. 6, and for the 811.5 nm line in Fig. 7. Similar behavior applies to the other atomic lines studied, but the cathode glow was too weak to establish the behavior of this ratio for the 476.5 and 488 nm ion lines. These numerical values of R_{NG} and R_{KG} are given in the same relative units, corrected for spectral sensitivity variations, for all lines.

The NG intensity decays slightly more gradually than

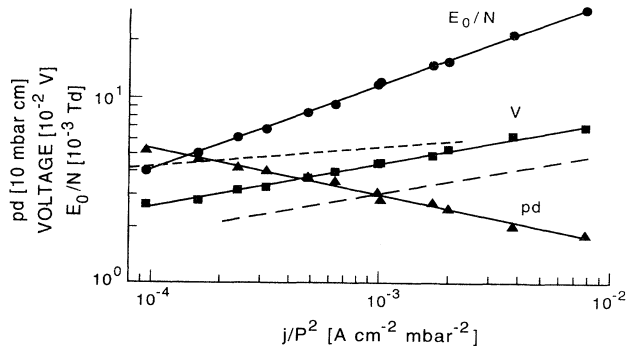

FIG. 5. Pd [mbar mm], voltage [10^{-2} V], and E_0/N [10^{-3} Td] as a function of j/P^2 calculated from four lines (476.5, 45.11, 750.3, and 811.5 nm), from 0.14, 0.27, and 0.67 mbar data.

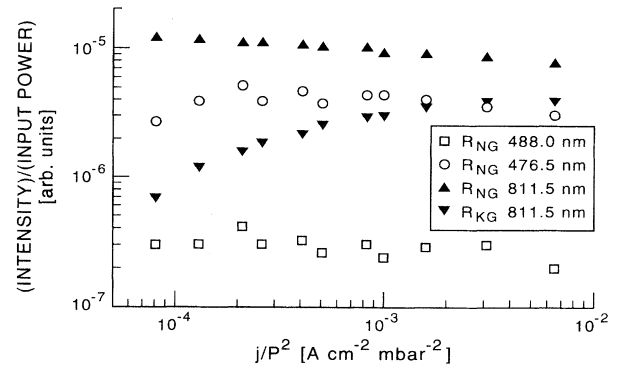

FIG. 7. Same as Fig. 6, but for three other lines.

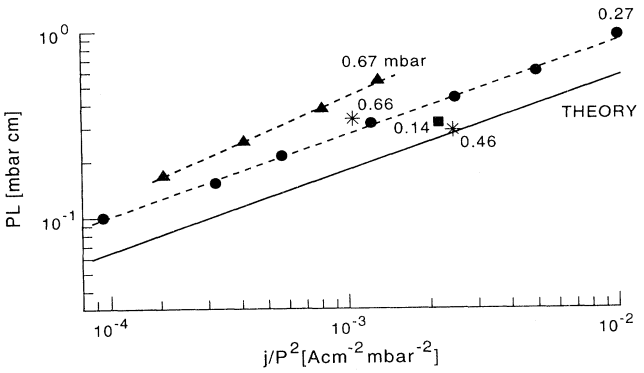

FIG. 8. LP vs j/P^2, where L is the decay length of the negative glow beyond the peak. The present data (solid points and dashed lines) are averages over four different wavelengths (476.5, 451.1, 570.3, and 811.5 nm), which had very similar L values. The data of Ref. [21] (*) is taken at 0.66 and 0.46 mbar, as indicated. The theoretical result of Ref. [10] (solid line) is the same at all pressures within the range studied here.

exponentially in the observed region beyond the negative glow peak, but we will approximate this as $\exp(-x/L)$ here. PL is plotted for different pressures as a function of j/P^2 in Fig. 8. It can be seen that their dependence on j/P^2 changes with pressure. This is in contrast to the Pd and PL_K which did not show a variation with pressure (Fig. 5).

IV. DISCUSSION

Based on reasonable simplifying assumptions, which are particularly appropriate in the space-charge-dominated "abnormal glow" cathode sheath region, at constant j/P^2 the values of E/n, the ion and electron energy distribution functions and the ratio of the ion and electron densities to the gas density are expected to be the same as any equivalent Px position, where x is the distance from the cathode [14,15]. Thus we might expect that V, Pd, PL_K, PL, R_{NG}, and R_{KG} depend only on j/P^2. In our measurements we found this expected dependence for all of these quantities except PL.

The increase of the voltage with j/P^2 in the present "abnormal glow" discharge is a general behavior, and several empirical relations have been found [15]. In our experiment $V \propto (j/P^2)^{0.25}$, which is similar to previous observations (e.g., Fig. 5). A gradual decrease in Pd with increasing j/P^2 (or voltage) is also a general behavior for all gases, although Pd does not always exhibit universal scaling (pressure independence) with j/P^2 [15]. In our case we found Pd proportional to $(j/P^2)^{-0.2}$, and it follows universal scaling for our pressure and j/P^2 range.

The cathode glow results from fast Ar^+ and Ar collisions with the thermal Ar atoms, where the fast Ar results from charge exchange. The ions undergo many charge exchange collisions in the sheath ($x=0-d$) [16], so their energy distribution at x depends strongly on the local E/N and the mean energy increases rapidly toward the cathode. For the same reason the flux and energies of fast Ar also increases rapidly toward the cathode. The threshold for exciting the observed Ar radiation is ~ 30 eV of laboratory frame energy, so the high-energy tails of the Ar and Ar^+ energy distributions are responsible. The weaker I_{KG} for the ion lines is clearly due to their much higher threshold excitation energy (~ 70 eV lab frame). Thus, $I_{KG}(x)$ is expected to increase rapidly toward the cathode, as observed. However, that $L_{KG}(x)$ is virtually independent of current was not expected and needs to be explained with a more detailed model. The increase in V and E_0/N, with increasing j/P^2, rapidly increases the high-energy tail of the distribution, so that R_{KG} rises with j/P^2 (Figs. 6 and 7).

The electrons gain energy in the sheath and deposit this in the negative glow, primarily by excitation and ionization. The energy gained by the electrons is $\int_0^d dx j_e(x)E(x)$ and total power $W=\int_0^d dx jE(x)=jV$, where $j=j_e(x)+j_+(x)$ with $j_e(x)$ the electron current and $j_+(x)$ the ion current. Thus, the fraction of the discharge energy delivered to the electrons, $F_e=\int_0^d dx[j_e(x)/j][E(x)/V]$, will be constant if the form of $j_e(x/d)/j$ and $E(x/d)/E_0$ in the sheath are invariant. $E(x)$ is known to decrease almost linearly from $x=0-d$, so $dxE(x)/V \cong 2(dx/d)(1-x/d)$ is a function of x/d that is essentially independent of j/P^2. Although the secondary electron yield at the cathode (γ) and the ionization efficiency in the sheath are expected to be voltage dependent, $j_e(x)/j$ is constrained to $\ll 1$ at $x=0$ and ~ 1 at $x=d$. Thus $j_e(x/d)/j$ is also relatively independent of j/P^2 and this leads to $F_e \cong \frac{1}{3}$ with very little sensitivity on the exact form of $j_e(x)/j$. Thus, our observation of $R_{NG} \cong$ const results from a nearly constant value of F_e.

The slow decrease of R_{NG} with increasing j/P^2 for the atomic lines in Figs. 6 and 7 probably indicates that a larger part of the electron energy goes into ionization versus excitation. As j/P^2 and the mean energy of the electrons increase, ionization is favored because the excitation functions of the 750.3 and the 451.1 lines from the $4P_1$ and the $5P_5$ levels of Ar rise rapidly at threshold and decrease slowly with increasing collision energy [16], whereas ionization rises almost linearly to peak at much higher energy. The excitation function of the 811.5 nm line ($4P_9$ level) is sharply peaked near the threshold [17], which would be consistent with a more rapid decrease of the R_{NG} (with increasing j/P^2) for this line. However, at our pressures radiation trapping causes higher ($3D$, etc.) Ar states to branch strongly into the $4P$ levels, whereas they decay mostly to the ground state at the low pressures where the optical excitation functions are measured. This apparently adds a broad high-energy tail to the 811.5 nm excitation, yielding a discharge behavior similar to the other lines. The excitation functions in Ref. [18] are consistent with this effect. R_{NG} for the ionic lines (476.5 and 488.0 nm) do not show this gradual decrease as clearly, perhaps because of the higher threshold for ionizing excitation or a small contribution from electron-ion collisions. However, it is clear that most or all of the ion line intensities are due to the electron collisions with Ar, because electron excitation of Ar^+ would

cause R_{NG} to rise approximately linearly with j/P^2.

The relative sizes of the KG and NG intensities for various Ar and Ar^+ lines depend on the ratio of heavy particle versus electron excitation cross section. The latter are well known [17], but may not apply directly to these higher-pressure discharges due to cascading. Some data regarding these heavy-particle cross sections are reported in Refs. [19,20], but the energetic neutral and ion fluxes and energy distributions versus x are not known. Here we do not attempt any comparison to cross-section data. As already noted, we chose to study two of these lines because their heavy-particle excitation in a high E/N discharge have already been measured and analyzed [11]. Our results for I_{NG}/I_{KG} appear qualitatively consistent with that study.

The pressure times lengths Pd and PL_k showed the same dependence on j/P^2 for all pressures studied consistent with similarity relations for the space-charge-dominated sheath region [14,15]. However, the negative glow decay lengths L and LP need further consideration. We observe approximately $L \propto (j/P^2)^{0.5}$, and attribute this primarily to the increase in the mean energy of the directed, energetic electrons entering from the sheath as j/P^2 increases. This is shown in Fig. 8, where our PL data are compared to PL measured in Ref. [21], and calculated from Ref. [10] using our measured V and Pd. The calculation predicts the same dependence on j/P^2 and a universal dependence of LP on j/P^2 as seen in Fig. 8. However, we observe different PL values for different gas pressures at a given j/P^2, as does Ref. [21] using 8 cm diameter electrodes with a 1 cm gap. The electric field in the negative glow is very small, so energetic electrons injected from the sheath largely diffuse as they lose energy in the negative glow. However, a relatively small negative glow field will cause some drift of these diffusing hot electrons, affecting L. Such fields could cause the scaling breakdown we observe, as they may be affected by the anode spacing or ambipolar diffusion, which can be different at different pressures. This decay length may also be affected by processes like Ar_2^+ recombination with slow electrons, which introduces additional pressure dependence. Since L for Ar^+ lines is the same as for Ar lines, excitation of Ar metastables and recombination radiation are not implicated. We believe that further study of the shape and the decay behavior of the negative glow may give information on the weak fields in the negative glow.

ACKNOWLEDGMENTS

The authors gratefully acknowledge Leanne Pitchford, A. V. Phelps, and B. Jelenković for helpful discussions, J. A. Neuman for his help with experiments, and L. Szalai for his help in evaluating the measurements. This work was supported in part by NREL Contract No. DD-11001-1.

[1] K. Rózsa, G. Stutzin, and A. Gallagher, J. Vac. Sci. Technol. A **11**, 647 (1993).
[2] R. A. Street, *Hydrogenated Amorphous Silicon, Cambridge Solid State Science Series* (Cambridge University Press, Cambridge, England, 1991).
[3] *Glow Discharge Spectroscopies,* edited by Kenneth Marcus (Plenum, New York, 1993).
[4] H. A. Phillips, H. L. Lancaster, M. B. Denton, K. Rózsa, and P. Apai, Appl. Spectrosc. **42**, 572 (1988).
[5] J. V. Sullivan and A. Walsh, Spectrochim. Acta **24**, 721 (1965).
[6] D. C. Gerstenberger, R. Solanki, and G. J. Collins, IEEE J. Quant. Electron. **QE-16**, 820 (1980).
[7] K. Rózsa, Z. Naturforsch. **35a**, 649 (1980).
[8] M. N. Hirsch and H. J. Oskam, *Gaseous Electronics,* Electrical Discharges Vol. 1 (Academic, New York, 1978).
[9] Z. Donkó, K. Rózsa, R. C. Tobin, and K. A. Peard, Phys. Rev. E **49**, 3283 (1994).
[10] I. Peres, N. Ouadoudi, L. C. Pitchford, and J. P. Boeuf, J. Appl. Phys. **72**, 4533 (1992).
[11] D. A. Scott and A. V. Phelps, Phys. Rev. A **43**, 3043 (1991).
[12] M. J. Dreyvestryn, Physica **9**, 875 (1938).
[13] B. N. Klyarfeld, L. G. Guseva, and A. S. Porkrovskaya-Sobleva, Sov. Phys. Tech. Phys. **11**, 520 (1966).
[14] F. L. Jones, in *Encyclopedia of Physics* (Springer, Berlin, 1956), Vol. XXII, p. 17.
[15] G. Francis, in *Encyclopedia of Physics* (Springer, Berlin, 1956), Vol. XXII, p. 70.
[16] J. E. Lawler, Phys. Rev. A **32**, 2977 (1985).
[17] J. K. Ballou, C. C. Lin, and F. E. Fajen, Phys. Rev. A **8**, 1797 (1973).
[18] Z. M. Jelenak, Z. B. Velikić, J. V. Bozin, Z. Lj. Petrović, and B. M. Jelenković, Phys. Rev. E **47**, 3566 (1993).
[19] V. Kempter, G. Riecke, F. Veith, and L. Zehnle, J. Phys. B **9**, 3081 (1976).
[20] A. V. Phelps, J. Phys. Chem. Ref. Data **20**, 557 (1991).
[21] B. M. Jelenković and A. V. Phelps, Bull. Am. Phys. Soc. **38**, 2359 (1993).